Rendering Imperfections

Marco F. Doerflinger*
Vienna University of Technology

Figure 1: Imperfections of the real world.

Abstract

Fast consumer graphics hardware enables graphic designers to create very detailed objects that are used in real-time applications. Even though it is common to utilize different kinds of mapping to imitate small geometry, it is not that common to imitate long term physical and chemical effects on surfaces. Nature is a dynamic space in which subtle interaction between molecules and other particles takes place permanently. Processes as these are for example oxidation, erosion and sedimentation. This paper discusses different methods to generate a more realistic impression by adding imperfection to a virtual environment. The presented approaches should ease the work of computer graphics artists. The document also explains the underlying natural phenomena and the psychological impact of modified scenes on test persons.

CR Categories: I.3.7 [Computer Graphics]: Three-Dimensional Graphics and Realism—Color, shading, shadowing and texture;

Keywords: rendering dirt, rendering dust, rendering scratches, weathering, imperfections, perceived realism

1 Introduction

One of the tasks of computer graphics is to create realistic virtual worlds. Because it is not possible to build a complete physical model of nature on a computer up to the present - chaotic processes[Gleick 1987] are not to 100% predictable - artists have to find ways to create believable abstractions. The visual system of humans can only process a limited data set. (see [Stone 2003] and [Nassau 2001]) This is the reason why it is important to find out which visual stimuli are adequate to produce the desired outcome at low costs.

An input that is significantly influencing the subjective accuracy of a virtual world is its imperfection. ”A real environment is unlikely to be pristine but will have accumulated dirt, dust and scratches from everyday use. Although human observers do not perhaps consciously take note of these phenomena, the absence of such features from the synthetic representation of that real scene may indeed affect the viewer’s perceived realism of the virtual environment.” [Longhurst et al. 2003] Longhurst et al. verify this in an experiment where photographs, ”clean” scene renders and with dirt and scuffs enhanced render images have been shown to participants (Figure 2). The results (Figure 3) show that the modified pictures are very close to photo-realism.

2 Exposition

To hand-paint effects such as dirt and scratches can often be very labor-intensive. [Dorsey and Hanrahan 1996] Following algorithms try to minimize the complexity of the working process. They are sorted by the initial data.

*e-mail: e0230635@student.tuwien.ac.at

Figure 2: Photograph and artistically enhanced render image. [Longhurst et al. 2003]

2.1 Process based Weathering Simulations

2.1.1 Simulation of Metallic Patinas

Dorsey and Hanrahan offer a method to create copper patinas (see [Hayez et al. 2005]). They use a stack of layers and a set of operators which can be applied to the surface. Each layer resembles a certain homogenous material. The attributes of the materials are for example shininess, roughness, diffuse and specular colors. There is also a thickness term which depends on position and there are two properties which control subsurface scattering ([Carr et al. 2003]).

Five operators are present. (Figure 4) Coat adds a new material layer of a certain thickness to the layer stack of the surface. Erode decreases the thickness of the layers one by one until it reaches the specified depth. One can imagine it as digging into the surface. Fill fills gaps in the material up to the given global height limit starting from the innermost layer. Polish removes hills in the material down to the given global height limit. Offset adds a new material layer like the coat operation does and then removes it partially by testing if it is covered by a given sphere.

Every operator is controlled by a texture map. This map contains information about the thickness of a material at selective points. The map itself varies over time. The thickness increases. Dorsey and Hanrahan also implement a simple scripting language to ease the handling of their system. The code example in Figure 5 shows different kinds of growth models. *ST* means steady thickening and is a linear model with a small amount of noise. *RD* stands for random deposition. It randomly generates particles that fall vertically until they hit the surface. An extension of this method is surface relaxation. It generates a smoother surface because the particles are placed at the innermost possible position in a certain radius. *BD*, ballistic deposition is very similar to the previous method. The difference is that the particles are depending on neighboring particles in the way that they stick to their edge. See Figure 6 for a better understanding.

2.1.2 Simulation of Washes and Stains

Dorsey et al. propose a method to simulate the flow of water over surfaces. The core of the approach is a particle system. The particles act like raindrops. This rain influences the appearance of a surface by washing away a small amount of material and transporting it to other points. This implies that there are two material classes. One group of materials consists of the accumulations on the object surface which can be replaced by the water. The other class holds only the surface material itself which is static.

Every material has its own properties. These properties consist not only of attributes which are important for the interaction with light but also contain parameters for the interaction with water. (Table 1) presents these parameters at a glance. (Table 2) and (Table 3) show the properties of the particle system and the environmental properties respectively.

2.2 Image based Simulations

2.2.1 Weathering using the STAF

The previous methods base on physical simulations and therefore do not require photographs as input data. Nevertheless these systems have a drawback. They are only applicable to a certain type of material or aging process. The following technique [Gu et al. 2006]

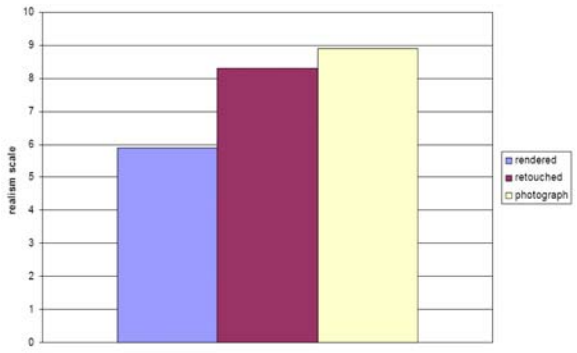

Figure 3: How does the image approximate reality (0-not at all, 10-very realistic). [Longhurst et al. 2003]

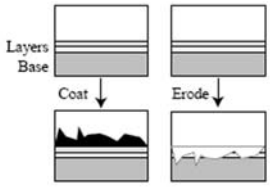

Figure 4: The coat and erode operators. [Dorsey and Hanrahan 1996]

```
new copper;
coat tarnish 1 0.35 texture(BD linear 1 20);
coat cuprite 2 1.2 texture(DPD linear 5 40);
coat marine patina 3 3.0 texture(BD linear 10 20)
coat marine patina 4 1.8 texture(DPD linear 20 40);
erode 0.5 texture(BD linear 5 20);
render maps;
```

Figure 5: Script for Copper Patinas in a marine environment. [Dorsey and Hanrahan 1996]

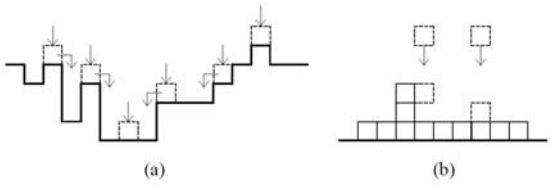

Figure 6: (a) Random deposition: The bent arrows indicate RD with surface relaxation. (b) Ballistic deposition. [Dorsey and Hanrahan 1996]

Material Properties		
	Properties	Notation
Material	Diffuse color	C_d
	Specular color	C_s
	Shininess	s
	Roughness	r
	Absorption	a
	Absorptivity	k_a
Deposits	Diffuse color	C_d
	Adhesion rate constant	k_S
	Solubility rate constant	k_D

Table 1: Attributes of the two major classes of materials: Base materials and loose deposits. Rate constants (properties beginning with k) are used in the differential equations controlling absorption of water and sedimentation of loose deposits (see Table 4). [Dorsey et al. 2006]

Water Particle Properties	
Attribute	Notation
Mass	m
Position	x
Velocity	v
Soluble material i	S_i

Table 2: Particle attributes. [Dorsey et al. 2006]

uses an underlying database with sets of time and spatially varying materials.

The capture device for the data acquisition is a rack in form of an icosahedron which holds 16 cameras and 150 light emitting diodes. Figure 7 shows the hardware. The custom design makes it very difficult to adopt the whole concept. Therefore it is more likely that other institutions use existing datasets.

The generated dataset is the base for a reflection model. Because this model represents a process that varies in time, a homogenous BRDF (See 3.1) is not appropriate. The function used in this case is an extension of a Spatially Varying Bidirectional Reflectance Distribution Function called TSV-BRDF. (See 3.2) The T is short for time and indicates that the function also varies temporarily. A minor weak point of this method is that it is not suitable for rough surfaces. For these cases a Time Varying Bidirectional Texture Function, short TBTF is the better solution.

One of the challenges that might occur when using a discreet dataset is that the images can not be used directly on arbitrary objects. The data has to be interpolated but in this case it is not appropriate to use a direct interpolation method. As you can see in Figure 8 double barycentric interpolation (as presented in [Vlasic et al. 2003]) does not produce acceptable results. There is a hard boundary between the dark and bright parts of the model and the highlights are not accurate as well.

The solution is given by the Space-Time Variance Factorization, short STAF. This interpolation method is independent of the used BRDF and thus can be applied to other representations of the function as well. There are different distributions of the parameters at every spatial location over time, so it is reasonable to seperate temporal variations from spatial ones. Exactly this is what the STAF

Environment attributes	
Attribute	Notation
Rain	$I_{w_{rain}}$
Sunlight	$I_{w_{sun}}$
Deposits	I_{D_i}

Table 3: Environmental attributes. [Dorsey et al. 2006]

Absorption and Deposition Process
Absorption
$\frac{\partial m}{\partial t} = -k_a \frac{a-w}{a} \frac{A}{m}$
$\frac{\partial w}{\partial t} = k_a \frac{a-w}{a} \frac{m}{A} - I_{w_{sun}}$
Sedimentation
$\frac{\partial S_i}{\partial t} = -k_{S_i} S_i + k_{D_i} D_i \frac{m}{A}$
$\frac{\partial D_i}{\partial t} = k_{S_i} S_i \frac{A}{m} - k_{D_i} D_i + I_{D_i}$

Table 4: Sedimentation equations. The top two equations control the absorption of water by the surface; the bottom two equations control the sedimentation of loose deposits. In this last set of equations, the subscript $_i$ is used to signify different types of deposits. S_i is the concentration of dissolved material in a water particle, and D_i is the concentration of material deposited on the surface. All other parameters and functions are described in Tables 2 and 3. [Dorsey et al. 2006]

model provides. It is defined by the following equations (1, 2):

$$p(x,y,t) = A(x,y)\phi(t') + D(x,y) \tag{1}$$

$$t' = R(x,y)t - O(x,y) \tag{2}$$

The parameters for temporal variations: $\phi(t')$ is a temporal characteristic curve. The definition of the curve depends on the acquired data set and therefore differs in respect to the underlying physical effect. For the measurement of the curve an estimated value is used and then approximated recursivly. $t' = R(x,y)t - O(x,y)$ is the so called *effective time* ([Gu et al. 2006]). It is a time value that differs between local positions. While t is the global time.

The parameters for spatial variations: $R(x,y)$ is the spatial rate, meaning that it describes the evolution speed of a certain spatial location.
$O(x,y)$ is an offset of the starting point in time. Positive values mean earlier in time.
$A(x,y)$ and $D(x,y)$ describe static SV-BRDFs (See 3.2). They are time independent and correspond to static patterns in the material, e.g. wood grain.

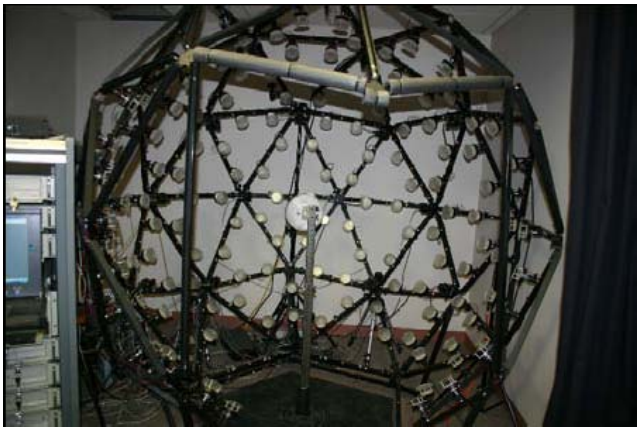

Figure 7: A photograph of the multi-light source multi-camera dome used for acquisition of the database of time-varying measurements. [Gu et al. 2006]

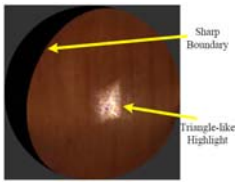

Figure 8: Barycentric interpolation. [Gu et al. 2006]

2.2.2

Wang et al. [Wang et al. 2006] present a method which significantly reduces the effort for image generation. As seen in section 2.2.1 a simulation based on linear interpolation does not deliver good results. So this technique also generates a non linear aging process with the advantage of very fast data acquisition.

The observation that points of a surface age in varying rates dependent on their spatial location, leads to the assumption that only one material sample contains enough information to interpolate the missing stages of weathering. The gained data can be transferred to arbitrary models or used to simulate the aging of the object on the captured image itself.

The user of the system has to distinguish between surface patterns and weathering effects manually. In the first step he plots the per pixel BRDF values of the image into an appropriate parameter space. A so called appearance manifold ([Wang et al. 2006]) is created. The model bases upon the assumption that the effects of aging can not decrease over time. Figure 9 shows this graph wherein the user has to associate weathering degrees with appearance states. The marking happens in image space $I(x,y)$ where the user can see the different weathering stages best. It is only required to mark the most weathered and the most unscathed parts on the texture.

A neighborhood space is created by utilizing the k- and ε-rule (See 3.3). The ε-value – which is a distance threshold – has to be calculated. To do so the system creates a vector by sampling the BRDFs of the point pairs of the k-rule graph over a set of viewing and lightning directions. After that the distance can be calculated. Therefore the vectors have to be transferred into logarithm space where the square distance is computed. (See [Matusik et al. 2003])

The elements of the user defined regions (the most and least weathered parts of the texture as described above) are separated from

the others to calculate an extended set of weathered points X_1. (3) shows the underlying formula as presented in [Wang et al. 2006].

$$X_1 = \{x_i | \phi(x_i, x'_0) > \lambda \Phi(X'_0, X'_1)\} \tag{3}$$

X'_0 and X'_1 are the user defined sets of the most intact and the most weathered sections of the material respectively. $\phi(x_i, x'_0)$ is the shortest distance along the connecting paths of the graph. x'_0 is the reference point to mesure the distance between x_i and X'_0 and thus is closest element to x_i of the set. λ is a threshold value to define the maximum extension of X_1. $\Phi(X'_0, X'_1)$ is the minimum distance between the sets. An extension of X'_1 is also created similarly.

$$\varphi(x) = \frac{\phi(x, x'_0)}{\phi(x, x'_0) + \phi(x, x'_1)} \tag{4}$$

To control the aging process a scalar is computed. It is the distance of an arbitrary point x to the least weathered set by the sum of the distances to the least and the most weathered set (4). Wang et al. advises against calculating the values for each frame seperatly because there is no spatial consistency between frames. The approach to calculate the data for an initial moment and then interpolate the values over the frames does not show natural behaviour either. The proposed technique is to calculate key frames and interpolate between them. To preserve the detail and to avoid repetitive textures the computation model includes an area around every pixel.

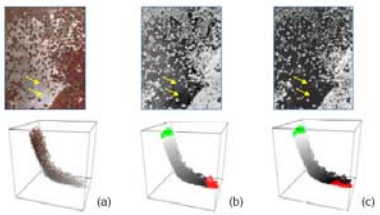

Figure 9: Appearance manifolds constructed from a rusted iron sample. (a) Diffuse image of the material sample, and the initial manifold. (b) Associated weathering degrees determined using Isomap reduction to 1D, exhibited in both the appearance manifold and the degree map. Two unweathered points (indicated by arrows) with different BRDFs are mistakenly assigned to different weathering degrees. (c) With user input, our technique assigns the same weathering degree to these two points. The red (green) set in (b) and (c) indicates the least (most) weathered points. [Wang et al. 2006]

3 Further Definitions and Formulas

3.1 BRDF

BRDF is an acronym for Bidirectional Reflectance Distribution Function. In its simplest form it has four dimensions, two for the angle of incidence and two for the angle of reflection.

$$f_r(\Theta_i, \phi_i; \Theta_r, \phi_r) \equiv \frac{dL_r(\Theta_i, \phi_i; \Theta_r, \phi_r; E_i)}{dL_i(\Theta_i, \phi_i) \cdot \cos\Theta_i \cdot d\omega_i} \tag{5}$$

E_i . . .incident irradiance
L_i . . .incident radiance
L_r . . .reflected radiance
Θ_i, ϕ_i . . .angles of incident ray
Θ_r, ϕ_r . . .angles of reflected ray
ω_i . . .solid incident angle

The equation in (5) describes a homogenous material without fluorescence, wavelength dependence, subsurface scattering (see [Carr et al. 2003]) or variations in space or time. Figure 12 shows the principles of a simple BRDF. Further readings which go deeper into detail of BRDF and extended versions thereof are [Nicodemus et al. 1977] and [Horn and Sjoberg 1978].

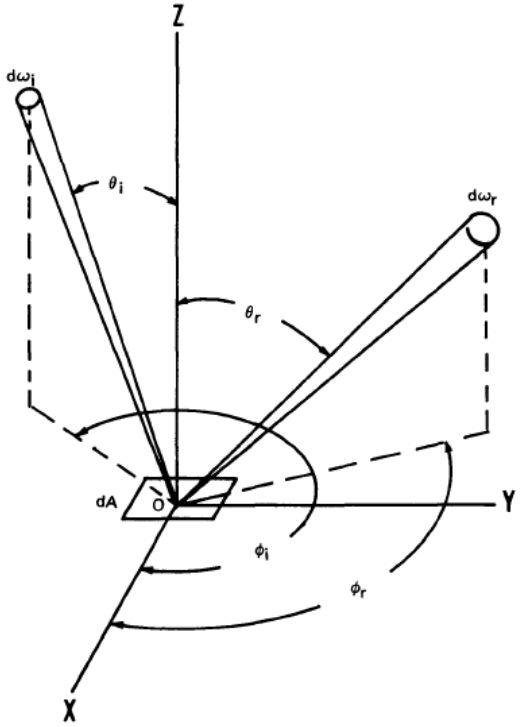

Figure 10: Taxonomy of appearance representation. The dimension of the most general description of light interacting with matter is reduced by adding more and more assumptions resulting in manageable functions like the BRDF. [Nicodemus et al. 1977]

3.2 SV-BRDF

Spatially Varying BRDFs include two more dimensions for the spatial location. The additional parameters allow the simulation of materials with surface patterns. Figure 11 gives a brief overview over different BRDF types and their dimensions.

Figure 12 shows a render of the Minerva of Arezzo using a homogenous BRDF. Figure 13 is a representation of the same object with a SV-BRDF. The spatially varying BRDF clearly reproduces the pattern of the surface of the real statue (Figure 14) while this is not possible with the homogenous approach.

3.3 Dimensionality Reduction

Tenenbaum et al. present a technique to filter out the outliners of huge datasets. They introduce the k- and the ε-rule (See [Tenen-

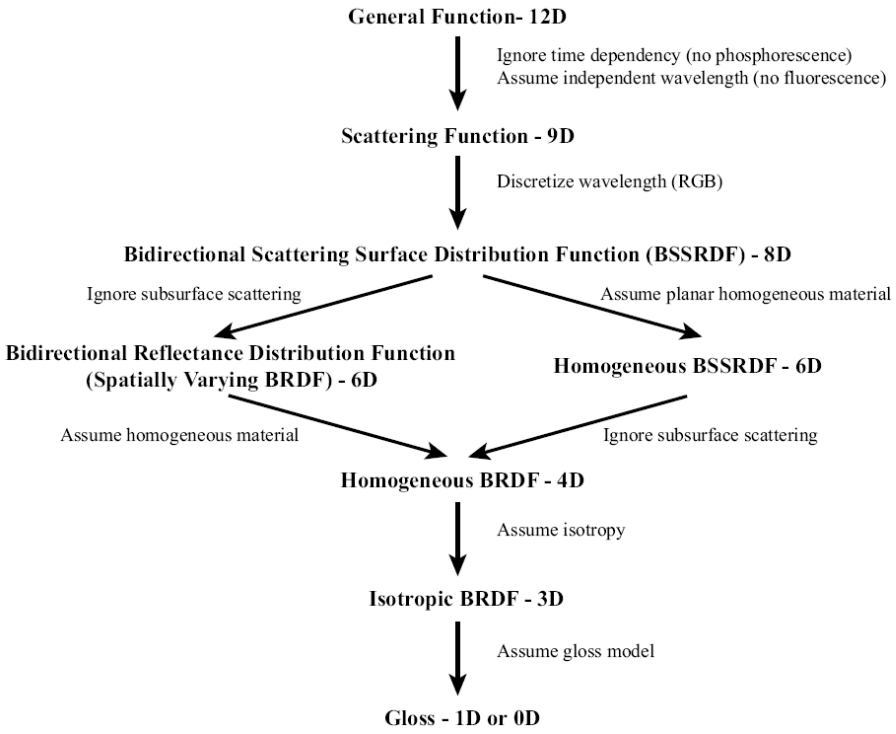

Figure 11: Taxonomy of appearance representation. The dimension of the most general description of light interacting with matter is reduced by adding more and more assumptions resulting in manageable functions like the BRDF. [Lensch et al. 2005]

baum et al. 2000]). By applying the k-rule one has to connect the k nearest neighbors of one point to form a graph. Points that are farther away than a certain threshold ε are then discarded.

4 Conclusion

As Longhurst shows in his work ([Longhurst et al. 2003]) there are several factors that influence the feeling or realism obtained by viewing a rendered image. One of these factors is the transfer of imperfections from the real to the virtual environment. Only a few studies in this field exist, so further research would help to find better ways to trick the human perception. Even Longhurst uses only 28 participants in the presented work, which produces an arguable significance. Nevertheless it is a good start.

There are two main groups of methods to generate imperfections in a virtual scene presented in this paper. The first type is based on physical models. ([Dorsey and Hanrahan 1996], [Dorsey et al. 2006] You have the freedom to script your own materials in nearly infinite ways but the problem is that the system covers only a small part of the whole lot of processes that can happen to different materials. You get a very accurate simulation for a very special case but it is not very likely that you generate good results with a patina generation algorithm if you want to let a virtual banana decay.

By contrast an image based system is applicable to most different cases of aging. The most difficult part in a working process with this model is the data acquisition. ([Gu et al. 2006], [Lu et al. 2007]) To get an accurate simulation you have to shoot many pictures of the model from many different viewing angles, illumination variants and stages in the weathering process. There are methods which work with single shot picture acquisition ([Wang et al. 2006]) but the visual correctness of the result is questionable.

Finally I want to give you some of the resulting images of the different methods. Figure 15 shows a result of the algorithm presented in 2.1.1. Another model based on physical equations is Figure 16. It is presented in 2.1.2. The image based models produce output as seen in Figure 17 and 18 and are presented in 2.2.1 and 2.2.2 respectivly.

References

CARR, N. A., HALL, J. D., AND HART, J. C. 2003. Gpu algorithms for radiosity and subsurface scattering. In *HWWS '03: Proceedings of the ACM SIGGRAPH/EUROGRAPHICS conference on Graphics hardware*, Eurographics Association, Aire-la-Ville, Switzerland, Switzerland, 51–59.

DORSEY, J., AND HANRAHAN, P. 1996. Modeling and rendering of metallic patinas. In *SIGGRAPH '96: Proceedings of the 23rd annual conference on Computer graphics and interactive techniques*, ACM Press, New York, NY, USA, 387–396.

DORSEY, J., PEDERSENY, H. K., AND HANRAHAN, P. 2006. Flow and changes in appearance. In *SIGGRAPH '06: ACM SIGGRAPH 2006 Courses*, ACM Press, New York, NY, USA, 3.

GLEICK, J. 1987. *Chaos: making a new science*. Penguin Books, New York, NY, USA.

GU, J., TU, C.-I., RAMAMOORTHI, R., BELHUMEUR, P., MATUSIK, W., AND NAYAR, S. 2006. Time-varying surface appearance: acquisition, modeling and rendering. In *SIGGRAPH*

Figure 12: Homogenous BRDF. [Lensch et al. 2005]

Figure 13: Spatially Varying BRDF. [Lensch et al. 2005]

'06: ACM SIGGRAPH 2006 Papers, ACM Press, New York, NY, USA, 762–771.

HAYEZ, V., COSTA, V., GUILLAUME, J., TERRYN, H., AND HUBIN, A. 2005. Micro raman spectroscopy used for the study of corrosion products on copper alloys: study of the chemical composition of artificial patinas used for restoration purposes. *Analyst 130*, 4, 550–556.

HORN, B. K. P., AND SJOBERG, R. W. 1978. Calculating the reflactance map.

LENSCH, H. P. A., GOESELE, M., CHUANG, Y.-Y., HAWKINS, T., MARSCHNER, S., MATUSIK, W., AND MUELLER, G. 2005. Realistic materials in computer graphics. In *SIGGRAPH '05: ACM SIGGRAPH 2005 Courses*, ACM Press, New York, NY, USA, 1.

LONGHURST, P., LEDDA, P., AND CHALMERS, A. 2003. Psychophysically based artistic techniques for increased perceived realism of virtual environments. In *AFRIGRAPH '03: Proceedings of the 2nd international conference on Computer graphics, virtual Reality, visualisation and interaction in Africa*, ACM Press, New York, NY, USA, 123–132.

LU, J., GEORGHIADES, A. S., GLASER, A., WU, H., WEI, L.-Y., GUO, B., DORSEY, J., AND RUSHMEIER, H. 2007. Context-aware textures. *ACM Trans. Graph. 26*, 1, 3.

MATUSIK, W., PFISTER, H., BRAND, M., AND MCMILLAN, L. 2003. A data-driven reflectance model. In *SIGGRAPH '03: ACM SIGGRAPH 2003 Papers*, ACM Press, New York, NY, USA, 759–769.

NASSAU, K. 2001. *The Physics and Chemistry of Color: The Fifteen Causes of Color*. John Wiley & Sons, Inc.

NICODEMUS, F., RICHMOND, J., HSIA, J., GINSBERG, I., AND LIMPERIS, T. 1977. *Geometrical Considerations and Nomenclature for Reflectance*. U.S. Government Printing Office, Washington, D.C. 20402.

SAILKO. 2006. Museo archeologico di firenze, minerva d'arezzo.

STONE, M. C. 2003. *A Field Guide to Digital Color*. AK Peters Verlag.

TENENBAUM, J. B., DE SILVA, V., AND LANGFORD, J. C. 2000. A global geometric framework for nonlinear dimensionality reduction. *Science 290*, 5500, 2319–2322.

VLASIC, D., PFISTER, H., MOLINOV, S., GRZESZCZUK, R., AND MATUSIK, W. 2003. Opacity light fields: interactive rendering of surface light fields with view-dependent opacity. In *I3D '03: Proceedings of the 2003 symposium on Interactive 3D graphics*, ACM Press, New York, NY, USA, 65–74.

WANG, J., TONG, X., LIN, S., PAN, M., WANG, C., BAO, H., GUO, B., AND SHUM, H.-Y. 2006. Appearance manifolds for modeling time-variant appearance of materials. In *SIGGRAPH '06: ACM SIGGRAPH 2006 Papers*, ACM Press, New York, NY, USA, 754–761.

Figure 14: A photograph of the real statue, taken at Museo archeologico di Firenze. [Sailko 2006]

Figure 15: A sense of time. On the left is a sequence of images showing the aging of a statuette. Time progresses from top to bottom. The larger image above illustrates the buildup of both the underlying smooth copper sulphide tarnish and the rough green patina. [Dorsey and Hanrahan 1996]

Figure 16: Simulated flows on a gargoyle. Rendering with flow patterns. [Dorsey et al. 2006]

Figure 17: Creating ephemeral patterns by adjusting rates. The bowl uses the burning wood dataset, and on the table is drying orange cloth. Control is provided by a virtual heat source. We start with the static appearance, gradually evolving into the Siggraph logo, and then into a fully charred and dry state. [Gu et al. 2006]

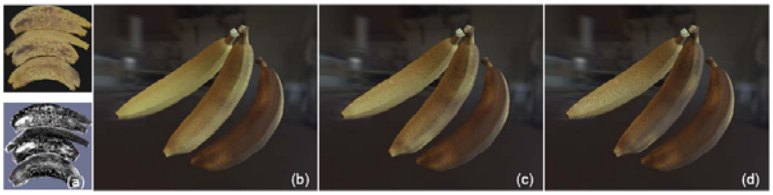

Figure 18: Three bananas at different stages of weathering. (a) The original sample and its degree map after analysis. (b)(c)(d) Rendering results of bananas under global illumination. The most weathered banana at the bottom is kept constant for reference. [Wang et al. 2006]